P-ISSN 2586-9000
E-ISSN 2586-9027
Homepage : https://tci-thaijo.org/index.php/SciTechAsia
Science & Technology Asia
Vol. 28 No.1 January - March 2023
Page: [136-151]
Original research article

Laboratory Experiments for Devising a Hybrid Seawall

Vaishnavi Dabir*, Kanchan Khare

Department of Civil Engineering, Symbiosis Institute of Technology, Deemed University, Pune 411062, India

Received 28 March 2022; Received in revised form 30 July 2022
Accepted 10 August 2022; Available online 20 March 2023

ABSTRACT

A seawall structure is the final line of defense for coastal conservation against erosion due to sea waves. The existing seawall design practices require dredging coastal resources such as sand or use heavy rubble mounds for construction. In this study, lab experiments to assess the energy dissipation performance of three types of seawalls is presented. The first set of tests are carried out on concrete blocks in armour layer, in the second set, geosynthetic encapsulating particulate material is studied. The experiments indicated that the surface properties, as well as fill properties, affect wave energy dissipation. Therefore, a hybrid seawall was devised combining the advantages studied in previous experiments. The locally available and highly permeable coir geotextile is incorporated along with the geosynthetic sandbags to form a novel geocomposite. The composite was tested for multiple orientations to determine that permeability, an essential property for wave energy dissipation, lies in the range of 0.02m/sec to 0.105 m/sec, which is very high. The experimental results indicate the possibility of pilot study for better understanding of performance of a sustainable composite seawall.

Keywords: Biomaterial; Geocomposite; Hybrid seawall; Hydraulic performance; Seawall

1. Introduction

Coastal erosion is defined as a phenomenon wherein the loss of material due to various reasons exceeds the supply of the material to it [1]. It can be a problem when it occurs across coastlines having human settlements. The beach formation process needs to be accelerated at such places by the construction of structures such as groynes, jetties, seawalls, etc., which need to be dealt with in varying ways. The coastal population is vulnerable in the absence of flood protection structures [1], and global warming will worsen the scenario considering the increase in mean sea level along with storm events [2]. The

***Corresponding author:** kanchan.khare@sitpune.edu.in **doi:** 10.14456/scitechasia.2023.12

shorelines are noticed to be fluctuating seaward or landward based on the shore environment and wave climate. [2-4]. A seawall is a shore parallel structure, which can be constructed to restrain the eroding shoreline.

For coastal protection, seawalls can be categorized as hard or soft depending on the materials incorporated for their construction. An alternative is called hard when it is constructed out of traditional heavy construction materials such as rubble, masonry, concrete, wood, etc. Soft technique options comprise afforestation and reforestation, beach nourishment, restoration of the dunes, and use of marine engineering technologies such as geosynthetics [5]. The traditional systems which include rubble mounds and concrete seawalls, have the advantage of higher structural stability due to better self-weight. The structures also have a long history of application thus instilling more confidence in the stakeholders. There is, however, a significant disadvantage associated with the traditional systems. One is the non-availability of massive rocks [6]. The alternative to this is concrete, which adds to the carbon footprint. The procurement of timber is also a threat to forest resources. The recent trend focusing on environmentally sustainable material alternatives and careful use of limited natural resources has increased the usage of geosynthetics in coastal protection [7]. This forms an ideal solution between having to use rubble mounds and concrete, wherein exploitation of natural resources is avoided, additionally making the entire system lightweight; this is beneficial for construction and handling of the entire system.

2. Background

2.1 Geosynthetics

Geotextiles are thin and lightweight materials used as a replacement for more expensive, massive, or permanent constructions. They can be engineered for the desired performance. At present, the types of geosynthetics used in the coastal environment are Geosynthetic Wrap around Revetments (GWR), Geotubes, and Geosynthetic Sand Containers (GSC). The selection of each synthetic geosystem depends on the economy as well as site conditions. Globally, research is in progress to evaluate the performance of geosynthetics in structures for case-specific conditions. Outstanding work for understanding the generalized behavior has been done by [8-12]. All these studies indicate the importance of the experimental study of scaled-down models to assess the behavior of the geosynthetic structure in the coastal environment. [13] discussed the effect of scouring on the stability of the bank protecting structures. A comparison of sandstone walls with geotextile wraparound revetments (GWRs) was performed. 2D Limit Equilibrium along with FEM modeling analyses was performed on a sandstone case study. Results suggested that GWRs have exceptional adaptability against differential settlement as well as scour erosion.

There is substantial variety in geosynthetics material, each providing a unique solution; therefore the possibility of its application in the coastal domain has huge potential for research. The prime advantage of these systems is the ease of handling and therefore the construction; they can be engineered for the desired purpose. Geosynthetics use in beachfront areas has exceptionally expanded in the current decade due to the aforementioned reasons. In the case of application of geosynthetics for coastal protection, the focus of research communities is to elucidate the science using techniques such as wave-structure interaction using experimental and numerical tools. [14-15] have discussed various problems with the geotextile tube technology with the help of a shore protection case study of Young-Jin

beach on the eastern coast of Korea. Two-dimensional limit equilibrium theory was used for stability analysis of the structure, and the results of the hydraulic model test are discussed. The seabed sand was observed to be gradually accumulated around the geotextile tube-covered areas. Seaweed accumulation was observed on the surface after one year of installation, indicating that any adverse effect on the environment is unlikely with the use of geotextile polymer material and it is unlikely to harm marine life. Corbella and Stretch [16] have shared experience on independent non-covered geosystems used as breakwaters, groynes, and beach nourishment structures. The toe of the geosynthetic structure needs to be designed appropriately to attenuate undermining. This is an essential measure to avoid settlement and ultimately sinking of the structure due to scouring. In South Africa, geotextile sand-filled containers have been deployed as coastal defense measures; however, uncovered geosystems are vandalized or damaged by sharp objects such as floating ship debris, and wood pieces. Thus, the prime disadvantage of geosynthetic systems is associated with anti-social behavior and mishandling of the system after it is constructed. In places where laws and regulations are stringent, the structure is likely to be successful. Additionally, geosynthetics in general face severe abrasion from marine sediments or armour rock. Therefore, a sustainable coastal material is studied as a composite with existing geosynthetic bag to form a hybrid seawall. Due to an abundance of coir in coastal regions, immediate reinstallation would be possible in the event of vandalism.

2.2 Experimental investigations

Research around the globe is focused on innovation in using geosynthetics in various forms. The behavioral predictions and investigations of such structures are still in their early stages. The largest geotextile market in the world is the Asia Pacific region, driven by China and India along with other countries [18]. While few scientists propose an output based on the experimental investigation of fundamental properties and structural stability under wave actions, others focus on inference from case studies. An extensive study is required to study factors affecting the stability of GWR and their interrelationship in order to gauge its long-term performance [12, 17]. Similarly, there is a need for innovation in geosystems focusing on effective wave energy dissipation and long-term performance before recommending it for application. Geosynthetics made up of natural sources are economical as well as biodegradable. The natural geosynthetics could replace the existing polymer-based geosynthetics either partially or completely [18].

In this study, the fundamental structural features which affect the hydraulic performance of hard/soft seawalls are studied experimentally. A composite seawall that could perform better than the conventional alternatives is proposed. A preliminary investigation of the hydraulic permeability, which is an essential property for effective energy dissipation on the proposed composite, is presented.

3. Material and Method

The experiments were performed in a wave flume with dimensions 0.5m width x 1m height x 10m length. An in-house wave-maker system was manufactured for the generation of waves. For the first experiment, a plunger-type wavemaker was set with a 2 hp motor and a camshaft for controlling the torque output. The wavemaker is capable of the generation of waves up to a wave height of 10 cm in a water depth of 40 cm. Flumes with lengths more than or equal to 30m are used for wave reflection, sedimentation studies, etc.[19-22]. The length of the current wave flume is suitable for studies on wave

overtopping and wave pressure on the seawall, which is the scope of the present study [12, 17, 23].

Energy dissipation is a function of surface friction, surface shape (on which the wave impounds), and porosity. Therefore, the experiments were divided into two categories. The first one focused on the hard armour alternative in which energy dissipation is a function of the shape of armour, surface friction, and energy loss due to the gaps between interstices of armour unit. As the shape of armour is a governing parameter for effective energy dissipation (Muttray & Reedijk, 2008; Karti 2018) - [24, 25], the first set of experiments focused on the effect of the shape of concrete armour on energy dissipation. When considering the shape of the seawall, the hypothesis is that a circular shape would result in repulsing of waves and the sharper shape would break the wave energy due to the gradually increasing area of the armour resulting in less overtopping for the same wave conditions. This principle is followed in seawall armours such as tetrapods, dolos. etc; hence, triangular and circular surface-shaped concrete armour layers were cast for the experiment.

The second experiment assessed the soft armour alternative which is a geosynthetic bag with encapsulated sand in which the wave energy is dissipated due to the fill material characteristics such as porosity, permeability, density, etc. Each of these properties is varied in the experiment by mixing sand with alternate non-reactive particulate material, in this case plastic shreds.

The field values of wave height and wavelength were obtained from the Indian National Centre for Ocean Information Services (INCOIS). The values were then scaled down to suit the wave flume in which the experiments are performed. As the aim of the experiment was to assimilate the dominant factors affecting the energy dissipation, a sample size of the seawall was decided considering the flume dimensions. The dimensions were scaled up and cross-checked for realistic field range by following the analytical design guidelines given by the shore protection manual (U. S. Army corps of Engineers, 1984) - [26]. It was decided iteratively to adopt a scale of 1:30 for the experimental program. Froudian similitude conditions were ascertained for the model. Only geometrical scaling down is possible for a flume scaled seawall; it is not possible to reduce the sand size diameter or the aperture opening size of the geotextile.

3.1 Experiment on hard seawall armour layer

In this set of experiments, the energy dissipation was assessed by study of wave overtopping on the seawall. Additionally, the surface pressure exhibited during wave run-up was recorded using a vibration sensor. The vibration sensor assembly is comprised of an Arduino sensor, which is a single-board microcontroller for sensing the vibrations due to wave breaking on the seawall armour. The circuit has digital and analog input and output pins which are interfaced with multiple breadboards and circuits. The sensor assembly was waterproofed with a plastic casing and silicone. The vibration frequency corresponding to 1000 waves was recorded.

Three alternatives of armour shape, triangular shaped concrete blocks (N1), curved shaped concrete blocks (N2), and randomly placed aggregates (N3), were compared with seawall with no armour (N4). Concrete blocks (N1 and N2) were cast with a concrete M25 grade mix of 1:1:2. The dimensions of the blocks are 7×7×7 cm. The outer layer of N4 was geotextile wrapped on a sand filter layer to prevent wash-off. The core of the seawall was built using clay compacted to its optimum moisture content (OMC) (Table 1).

Table 1. Geotechnical data for clay used in the seawall core.

Physical properties	Values
Specific gravity	2.05
Liquid Limit	28.9%
Plastic Limit	9.55%
Dry unit weight	16.08 kN/m^3
Wet unit weight	17.69 kN/m^3
Toughness Index	9.04
OMC (%)	8

The filter layer was formed using locally available river sand. Following the recommendations given by [16], first-class bricks were used for the toe protection and 15.8 Kg of rock for the filling; the calculations were based on volume and density (Table 2). The base of the seawall was made up of plywood, with dimensions of 0.485m x 0.85m. The plywood covering the back was 0.50 m in height and 0.485 m in length.

To ensure that the model stays sturdy against the water load and the wave impact, the back of the seawall was cast with plain cement concrete PCC (1:2:4). The cement sand composition of 1:2 was adopted in the mix. The experimental setup is shown in Fig. 1. The complete seawall was built in situ with the help of boulders (random sized) laid as a backfill. The core was compacted considering its maximum dry density (MDD). A layer of geosynthetic material was used to separate the core from the filter layer. The topmost armour layer was randomly stacked. Post assembly of the entire model, the sensor assembly was installed to measure the impact of the wave on the armour layer. The seawall was constructed with a slope of 1:1.5. A filter layer was provided to avoid the in-situ piping of the soil. Soil may get washed off due to water ingress and improper contention of soil, resulting in the collapse of the structure.

Table 2. Material calculation for the seawall model.

Layer	Dimension (m)	Volume (m3)	Weight (kN)
Core	0.1*0.15*0.485	0.0072	127.29
Rock Fill	0.08*0.12*0.485	0.01	154.94
Armour	0.12 *0.18 *0.485	0.05	784.53

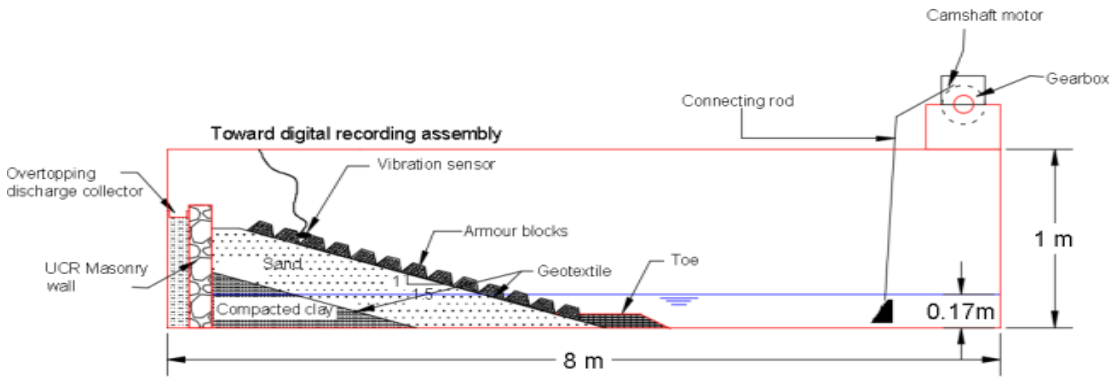

Fig. 1. Experimental setup for hard seawall (concrete armour).

For absorption of the re-reflected waves, and for turbulence control, a turf was provided near the toe of the seawall.

For the measurement of overtopping discharge, a rectangular acrylic channel was constructed connecting the seawall berm. After collecting data on pressure exhibited on the surface in terms of vibration frequency for 1000 regular waves, the overtopping discharge for 100 waves is measured by increasing the water depth from 40 cm to 60 cm and increasing the

wave period in stages from 3 seconds to 1 second for a dynamic attack of the wave over the structure.

3.2 Experiments on soft seawall armour layer

For the second set of experiments, a popular soft armour alternative made up of geosynthetic sandbags (GSB) was incorporated. Energy dissipation of soft alternatives can be measured in two ways. Firstly, it is possible to calculate wave reflection from the structure; for which the flume length should be at least three wavelengths long. Secondly, it can be assessed by measuring absorption and drainage within the structure. Therefore, with the available flume length, it was possible to measure energy dissipation by absorption. Hence, to measure the pressure due to run-up exhibited on the surface of the seawall due to the gradation and density of fill material in the soft alternative, the usual fill of sand in GSB was replaced in proportions with plastic waste shreds. This was done to replace sand with any other particulate reactive nature that could be tested to see if any other material apart from sand can be used in the geosynthetic as fill material.

The fill ratio of the sandbag was varied by adding plastic in 50%, 65%, and 80% proportion to sand, and the energy dissipation performance was recorded. A new wave maker was devised for this experiment by designing a flap-type wavemaker using the ratio of target wave height (H) to stroke (S_0) of the flap at a desired water depth kh using Eq. (3.1).

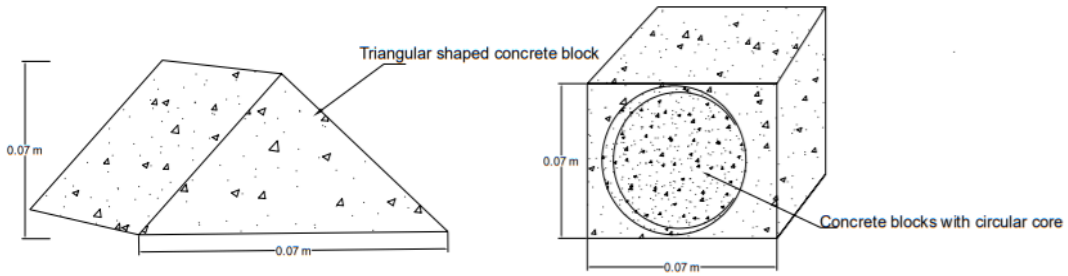

Fig. 2. Concrete armour shapes for hard seawall.

$$\frac{H}{S_0} = \frac{4\sinh^2 kh}{\sinh 2kh + 2kh}. \tag{3.1}$$

The power required to generate the wave was calculated using Eq. (3.2)

$$\frac{P_0}{\left(\frac{\rho g h S_0^2}{T}\right)} = \frac{\pi}{kh}\left(\frac{\tanh kh}{\sinh 2kh + 2kh}\right)\left[\sinh kh + \frac{1}{kh}(1-\cosh kh)\right]. \tag{3.2}$$

The power required was only 0.5 hp as compared to the motor capacity of 2 hp. Hence, a higher degree of control was possible for wave generation using the flap-type wavemaker. The pressure on the seawall was measured using a pressure transducer with measuring range of 0-300 millibar. The assembly consists of a diaphragm with a stainless-steel face connected to a flexible tube which was attached to the pressure transducer using a flexible tube filled with viscous fluid. The diaphragm resonates with each pulsating wave, resulting in pushing oil contained within the flexible tube which is sensed by the transducer. The transducer then transmits the pressure in terms of voltage, which is displayed on a digital indicator in

millibars. The fill material in this experiment was beach sand procured from the west coast of India (Mumbai). The sand was tested in the lab for its grain size properties and with a D_{90} of 1.5 mm (Fig. 3). The geobags and the filter layer sand geosynthetic bag incorporated in the field was around 0.5 cubic meters. The scaled-down dimensions of the sandbag were, therefore, determined to be length = 26 cm, breadth = 13cm and height = 5.2 cm.

The mass of mix to be filled into the sandbags was determined using volume and density calculations. Each of the layers of seawalls was separated using a geotextile with properties mentioned in Table 3 to prevent the intermixing of layers.

Table 3. Characteristics of the geotextile used (non-woven needle punched).

Properties	Values
UV Resistance	70% at 500 hrs. of exposure
Aperture Opening Size (AOS)	less than 75 micron
CBR Puncture Strength	3110 N
Trapezoidal Tear Strength	450 N
Grab Tensile Strength	1110 N
Grab Elongation	> 50%
Water flow	50 lit/(sqm/sec)

As a fill material, HDPE plastic shreds, which were by-products of the electrical insulation, were procured to be used as a substitute in proportion with the soil. To assess the effect of utilization of plastic shreds in the sandbag on energy dissipation, the proportion of 50% (P_{50}), 65% (P_{65}), and 80% (P_{80}) of plastic fills to sand fill was incorporated. Three types of plastic shreds with varying densities were selected for this study. Fig. 4 shows white-colored shreds (A), Black colored flaky structured plastic shreds mixed with white-colored shreds (B) and black-colored flaky structured plastic shreds (C). All the plastics are High-Density Polyethylene. The grain size analysis for the encapsulated sand samples A, B, and C with varying fill ratios viz. P_{50}, P_{65}, and P_{80} are shown in Fig. 5.

Fig. 4. Plastic shreds used as fill material.

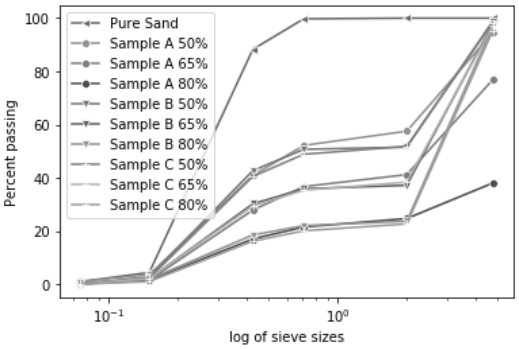

Fig. 5. Grain size analysis of HDPE shreds.

Fig. 6 shows the values of coefficient of uniformity (Cu) for all the samples and the coefficient of curvature (Cc) values of the same set. The sand used in this study had a coefficient of uniformity (Cu) of 1.97. and those of all plastic mixes are in the range of 10 to 13. The coefficient of curvature (Cc) of pure sand is 0.97 (Fig. 6), whereas that of plastic is in the range of 0.43 to 4.85. The coefficient of curvature value for pure sand is nearing unity. The density values of mixes using relative density were calculated as follows:

- Sample A – 0.633 gm/cm^3,
- Sample B – 0.543 gm/cm^3,
- Sample C – 0.400 gm/cm^3.

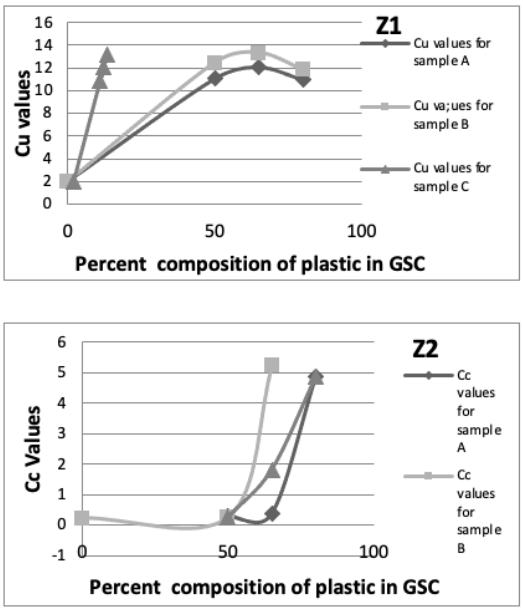

Fig. 6. Coefficient of uniformity and coefficient of curvature versus percent composition of plastic for all three samples in Zone 1 (Z1) and Zone 2 (Z2).

The variation in the coefficient of uniformity for the sand samples with the increasing plastic percentage (P_{50}, P_{65}, and P_{80}). For samples A and B both, the value of Cu is the maximum for an 80% fill proportion. Sample C showed the variation of coefficient of curvature in the same range despite the increase in the percentage of plastic. The coefficient of Uniformity (Cu) is a measure of the particle size range.

$$Cu = \frac{D60}{D10}, \tag{3.3}$$

$Cu = 1$ for uniformly graded soils, greater than 4 for well-graded soil, and for sand, the value is greater than 6. The soil type used in this study can be categorized as sandy gravel based on the range of the coefficients. The coefficient of curvature (Cc) is the shape of the particle size curve.

$$Cc = \frac{(D30)^2}{D10 \times D60}. \tag{3.4}$$

For a well-graded soil, $Cc = 1$ to 3.

For the plastic-sand mix fill, irrespective of the proportion of plastics, the overall Cu value remained very high; greater than 8 (Fig. 6). The Cc values showed a sharp increase with the increase in the plastic composition with the sand. Overall, the mix gradation for Sample B with a 60% plastic to sand ratio showed a well-graded range. The assembly was set up as shown in Fig. 7. Zone 2 (Z2) is the middle portion of the seawall and Zone 1 (Z1) is at the top 1/3rd portion of the seawall.

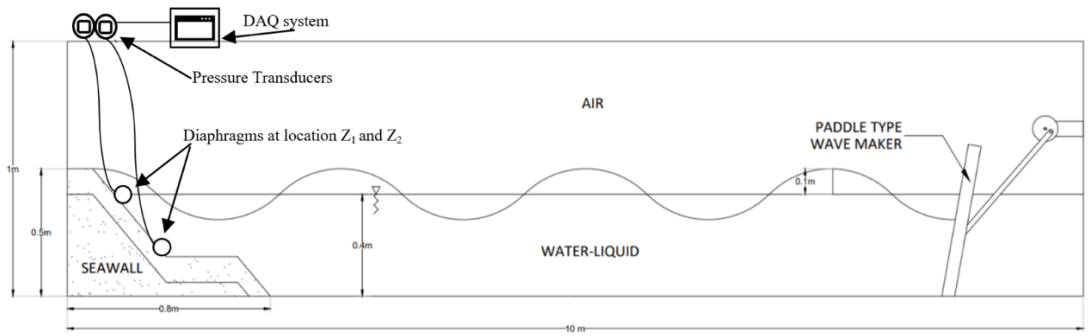

Fig. 7. Set up for soft seawall – geosynthetic sand-plastic mixture filled bags.

3.3 Experiments on the hybrid alternative

With the preliminary set of experiments on the hard and soft armour alternatives for energy dissipation, it was noticed that the soft alternatives provide ease of handling and address the perspective of being a relatively affordable solution. The prime factor for a hydraulically

efficient soft alternative structure is its permeability. The locally available and highly permeable coir geotextile was incorporated along with the geosynthetic sandbags to form a geocomposite. As the first step to working towards the solution, an evaluation of the effect of orientation of the composite structure on its permeability was conducted.

To estimate permeability, the method proposed by [28] was used. The size of the sandbags and sand rolls was kept constant. Sandbags of dimensions 0.5m × 0.2 m × 0.1m were utilized in this study. The composite was installed ensuring the occupancy of the entire width of the flume assuring the flow of water only through the structure and not through the gaps at the sides of the structure and the wall. The sandbag was filled up to 80% of its volume capacity with sand as recommended by (Dassanayake & Oumeraci 2012). The coir was rolled onto a diameter of 10 cm to match the size of the geosynthetic sandbag thickness. A total of 20 tests of different configurations were performed in this test program. Variations to the placement and positioning of the coir and sandbag were performed, resulting in the variation in the number and size of gaps in the composite structure. Each test was repeated four times, and the average value of permeability (k) for each orientation was noted.

As shown in Fig. 8, the head of water ($H1$) was maintained constant at the upstream of the flume. The downstream head ($H2$) for each orientation was measured manually. The difference of head $\Delta H = H1 - H2$ was noted. Length (ΔL) is the inclined distance of the width of the structure from the upstream to the downstream. It was measured to work out the hydraulic gradient (i) for each of the observations. The time required to acquire a set volume of (0.0162 m^3/sec) was recorded, and the difference of head for determination of the permeability that time was noted. Thereafter, the permeability k was computed using the Darcy's Law which signifies the macroscopic equivalent of Navier-Stokes' equations of motion for viscous flow. Based on the law, in the current experiment, the velocity head between the soil grains is neglected. The flow conditions are kept laminar. It is assumed that the flow is uniform and horizontal at all the points between the interstices of the vertical section of the structure. Water, as well as the porous medium, is assumed to be incompressible. An equation to determine the horizontal flow through stratified media is not applicable due to non-uniform layers and mixed placements of the composite. Hence, in the current method, an attempt is made to study the effect of orientation of the composite material on overall permeability of the composite.

Frontal view of Orientation O15

Side view of Orientation O20 – Randomly placed composite

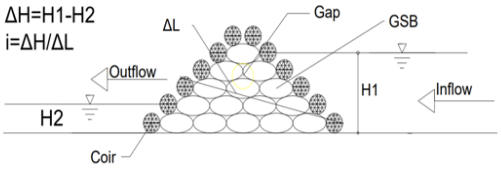

Permeability setup in the flume

Fig. 8. Composite materials and permeability measurement setup.

Table 4. Schematic configurations of the composite seawalls for hydraulic study.

Orientation	Side View	Orientation	Side View	Orientation	Side View	Orientation	Side View
O1		O6	Gap	O11		O16	Gap
O2	Gap	O7	Gap	O12		O17	Gap
O3	Gap	O8	Gap	O13	Gap	O18	
O4	Gap	O9		O14	Gap	O19	
O5	Gap	O10		O15	Gap	O20	

4. Results and discussion

In the first set of experiments, the behaviour of the concrete blocks of two distinct shapes (N1 and N2) in response to the wave impact was investigated experimentally to infer the energy dissipation due to shape of concrete blocks. These two cases are compared with classic rubble mounds as well as to the no armour condition. Table 4 shows the schematic configurations of the composite structures studied in the experiment. Fig. 9 shows frequency readings for 1000 waves simulating storm events for both the concrete armour shapes. The runs for N3 and N4 were limited to 500 waves due to displacement of aggregates in N3 and visual distortion in the shape of N4 observed

during the runs. The run had to be terminated before completing 1000 waves for N3 and N4 (Fig. 9). The distortion had materialized under the filtering geotextile, which separated the sand filter underlayer. The sand was subjected to drag and lift owing to the continuous movement of water by the dynamic impulsive waves. Thus, it can be stated that a seawall with N1 (triangular shaped concrete blocks) and N2 (curved concrete blocks) type armour has a better capability to sustain the wave attack as compared to a rubble mound or no armour condition and showed better stability.

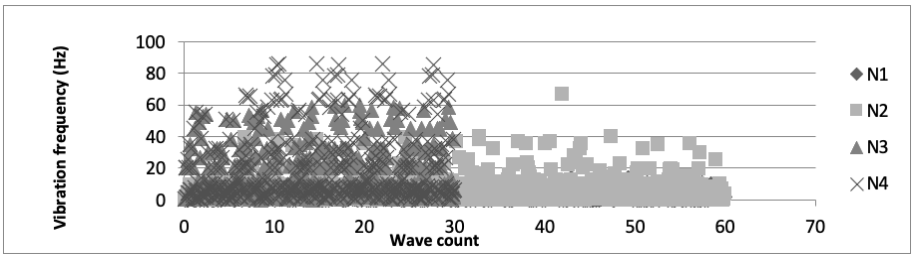

Fig. 9. Wave energy dissipation analysis for all variations.

The vibrational frequency experienced by the structure will be high if the wave climbs on the seawall with no obstructions. This was observed with the no armour condition, wherein the highest frequency was recorded. Table 5 shows the highest and lowest frequency obtained under the same wave characteristics, a constant Iribarren number of 0.92, and a varying armour shape. The breaking index γ value was 0.588 and the wave steepness was 0.45. As the sensor assembly is mounted at 25 cm from the top, the energy dissipation could be measured by recording readings of the frequency of breaking waves running up on the seawall. It can be inferred from Table 5 and Fig. 9 that the lowest frequency experienced was with N1 which is a triangular-shaped armour. Since the wave energy breaks down in the process of running up over the seawall, the sensor senses the lesser amount of water and also with lower intensity; thus lesser value of vibrational frequency is recorded on the seawall with N1 type armour. This siginfies wave energy dissipation due to the surface properties of seawall armour. Thus, the hypothesis that the gradually increasing surface area would dissipate the wave energy is positive.

Table 5. Frequency results for a wave height of 0.10 m, wavelength of 0.22 m, and a water level of 0.17 m.

Frequency (Hz)	N1	N2	N3	N4
Maximum	14020	40080	6000	86000
Minimum	46	95	200	360

The overtopping discharge was collected for 50 waves and the discharge collected for all variations can be ranked as N2<N1<N3<N4. The variation of N4 and N3 has again shown poor performance as compared to concrete hard armour alternatives. Fig. 10 shows the comparison of overtopping discharge to the vibration frequency and it can be noticed that for triangular-shaped armour N1, the vibration frequency experienced is the least out of all the alternatives tested; however, it has a comparatively higher overtopping discharge collected than the curved shaped armoured seawall. The reason for the lower overtopping also could be due to the random arrangement of the faces of the blocks.

The overtopping and vibration frequency followed polynomial equation with a degree two. It can be given as

$$O_d = 9E-08vfr^2 - 0.005vfr + 380.73, \quad (3.5)$$

where, O_d = Overtopping discharge in cubic centimetres, vfr = Vibrational frequency in H_z, R^2=0.9658.

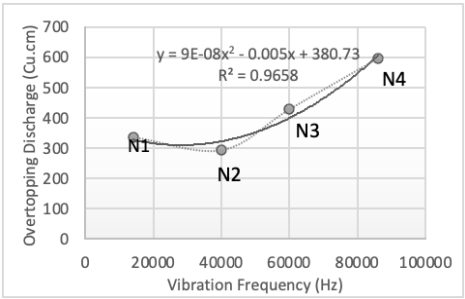

Fig. 10. Overtopping discharge versus maximum vibration frequency.

The alternative N4 (no armour) underwent erosion and settlement and ultimately lead to the distortion of the frontal face of a seawall. Thus, the importance of the armour layer for wave energy dissipation is highlighted. The toe of the seawall is essential for achieving stability against sliding. In the current experiment, burnt clay bricks were arranged at the toe of the structure. This helped to break the incoming waves, and also reduce the turbulence of re-reflected waves, which is a prime concern in short wave-flume studies, as suggested by Hornsey et.al (2011) - [27]. Thus, it implies that the use of a dense yet porous medium in the toe layer of the seawall may prove to be efficient for effective energy dissipation. The visual impact of wave overtopping and reflection is represented in Fig. 11.

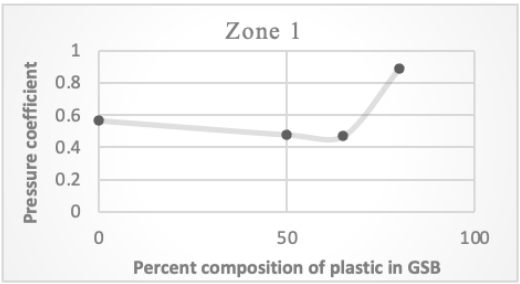

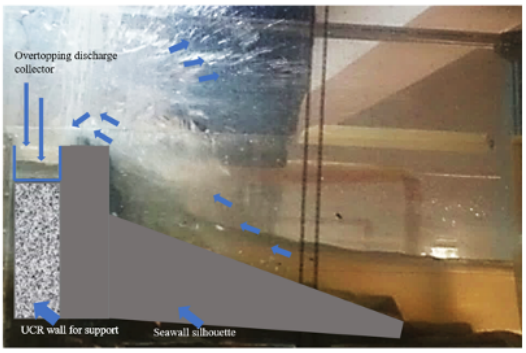

Fig. 11. Visual representation of wave impact and overtopping.

For the soft alternative, in the second set of experiments, the energy dissipation was measured as the pressure exerted on the surface as a function of fill characteristics during the wave run-up. During the relative density test of the plastic shreds mix A, B, and C matrix, A and C floated up due to vibration and sand settled down. This was due to less mass density of the particulate matters. Therefore, only mix B was used for encapsulation in 50, 60, 80, and 100% plastic to the sand ratio for the wave pressure analysis.

The values of pressure coefficients obtained in Zone 1 and Zone 2 of the seawall for the different percent plastic to sand composition against regular wave impact are shown in Fig. 12. The pressure coefficient is calculated by the pressure head in front of the seawall. Pressure readings obtained from sensors in millibars were converted to kg/m^2 (1millibar=10.20kg/m^2) tocalculate pressure coefficient.

$$P = \frac{pressure\left(kg/m^2\right)}{\rho g h}, \quad (3.6)$$

where,
P = Pressure coefficient (dimensionless), ρ = density of water kg/m^3, g = gravitational accelaration (kg/m^2), h = depth of water in front of the seawall (m).

In Zone 1 which primarily experiences the impact force of wave nappe and wave breaking pressure, the pressure value was reduced slightly with the increasing proportion of plastics in the seawall. However, there was a significant rise when the percentage of plastic was increased to 80%. This was because of the lesser density of the GSB fill matrix at 80% plastic to 20% sand compositions. For the wave energy to be dissipated successfully, the density of the matrix of the structure is of vital importance owing to the stability of the structure.

In the experiments, the 100% plastic GSB floated in the flume experiments and thus results of pressure were discarded. As far as Zone 1 is concerned, the 60% plastic filled with GSB showed excellent results of pressure dissipation. In Zone 2, the pressure exerted on the base of the seawall can be noted. With a longer wavelength, wave impacts with higher energy at the bottom of the flume. Thus, the variation in Fig. 12 shows that with the increase in fill ratio of plastic, there is lesser pressure experienced at the base of the seawall infused with plastic shreds. This could be due to the voids ratio of the fill material, wherein the water can flow through the voids and thus dissipate energy due to the movements through the interconnected spaces. It can be observed that the pressure values decreased with the increase in plastic shreds in Zone 1.

Owing to the advantages of soft alternative over hard, a preliminary experiment on finding the permeability of a geocomposite incorporating locally available coir roll along with geosynthetic sandbags was tried for 20 unique orientations as tabulated in Table 6. Out of the multiple orientations tried out in the experiments, in the model orientations with coir as the first layer of the structure, a faster flow of water was observed. However, in the reverse case, that is of sandbag as the first layer, a comparative resistance to seepage of water through the structure was observed.

Table 6. Permeability of the orientations.

Orientation	k (m/s)	Orientation	k (m/s)	Orientation	k (m/s)	Orientation	k (m/s)
O1	0.022	O6	0.042	O11	0.043	O16	0.050
O2	0.068	O7	0.039	O12	0.078	O17	0.037
O3	0.059	O8	0.032	O13	0.042	O18	0.029
O4	0.046	O9	0.039	O14	0.034	O19	0.033
O5	0.051	O10	0.091	O15	0.047	O20	0.105

This is because of the disparity in voids ratio of the frontal face of the composite, and thereby the porosity of the composite structure. Also, the density of coir rolls is much lighter than that of the geosynthetic sandbags; hence, it would be ideal to have coir rolls submerged under the GSB for stability.

The highest value of the coefficient of permeability is obtained for orientation O20. This was because, in O20, the geobags and coir rolls were dropped at random, leading to the creation of larger-sized gaps in the structure. The least permeability value was obtained for variation O1 which is 0.02 m/sec followed by O2, as the water was by-passed via only the small side gaps around the GSB and coir. It was observed for all the runs that the water is first absorbed by the interstices and voids in the coir roll itself and then passed out of it. Overall, it was observed that the permeability of the geocomposite is dependent on the engineering property viz. porosity and permeability of the frontal facing armour material.

The porosity of seawall directly affects the permeability of overall structure. A permeable structure results into decrease of kinetic energy due to reduction of wave

development and wave reflection. The roughness of the armour results in decrease in wave energy, wherein it breaks in the interstices of the particulate matters encapsulated in the geosynthetic or that of coir rolls. In the case of a composite seawall, the multiple obstructions provided due to openings and gaps between structures as well as porosity of the structure, would aid wave energy dissipation. For a seawall, therefore, permeability of the structure is an essential parameter.

5. Conclusions

The objective of this study was to observe the prime factors affecting seawall performance in the hard and soft alternatives, thereby forming a basis for the selection of materials and devise a hybrid seawall.

In the first experiment, the aim was to assess the effect of variation of armour layer shapes on the hydraulic performance of the seawall. In this set, the hard seawall structure was constructed with a clay core, geosynthetic filter layer, and a concrete armour layer with distinct shapes. It was observed that noticeable wave energy dissipation was achieved by randomly arranged triangular concrete blocks. This was because the energy could be reduced due to the increased surface area of the triangular armour shape. However, the overtopping performance of the curved-shaped blocks was higher as compared to the triangular-shaped armour. This was due to the fact the curved-shaped armour returned the waves into the seaward side owing to its shape, thus resulting in lesser overtopping. Thus, the N1 triangular shaped armour would be the ideal alternative considering its ability to reduce the force exerted by the wave on the seawall, thereby imparting higher stability to the structure. For high-tidal zones, the wave is suspected to overtop the structure in storm events; hence, a curved shaped seawall armour was studied considering possibility to avoid flood events. It was also noted that the wave energy can be reduced considerably by providing a porous toe layer. It was observed that the energy dissipation is 83.8 %, 53.5 % and 30.25% more for triangular shapes, rounded rubble, and randomly placed aggregates, respectively, as compared to no armour layer arrangements.

In the second set of experiments, geosynthetic sandbags were tested by varying the fill material in the geosynthetic bag in percent composition to the volume of sand. It was inferred from the results that the incorporation of alternate material is possible for increasing the efficiency of the geosynthetic sandbag for wave energy dissipation. Such bags could be used as river bunds for river training works, or at the inner harbour area for places of mooring of ships. Managing plastic waste is an issue that demands attention and possibilities for alternate uses. Thus, the incorporation of shreds in sandbags will boost many small-scale, shredding entrepreneurs. Additionally, the possibility of reducing the use of dredged sand can be achieved by the utilization of engineered alternatives to develop a high-functioning armour layer.

Finally, based on the results of the previous two sets of experiments, a hybrid seawall structure was devised with an advantage of a higher voids ratio, permeability, and surface roughness which aid energy dissipation. The locally available coir geotextile was rolled and stacked with geosynthetic sandbags to form a geocomposite. As a preliminary investigation, the most important hydraulic property, i.e., the permeability of this composite, was determined in the flume. The placement of the composite had very little effect on the overall permeability; the standard deviation of the results is only 0.02. The mean permeability value is 0.04 m/sec; such high permeability would result in quicker energy dissipation due to the hybrid combination. As a future scope, wave reflection study of proposed hybrid

seawall can be carried out for assessing the possibility of deploying a sustainable coastal protection structure.

Acknowledgement

This work is an output of Student Research Project-SIU-SRP/1139 and the authors are grateful to Symbiosis International (Deemed University) for the financial and infrastcructural support.

References

[1] E.W. Reckziegel, J. Weschenfelder, and T. Bazzan, "Avaliação do risco de inundação do Lago Guaíba e Delta do Jacuí, Rio Grande do Sul/Brasil," Rev. Gestão Costeira Integr., vol. 19, no. 4, 2019, pp. 221-43.

[2] A. Kumar, A.C. Narayana, and K.S. Jayappa, "Shoreline changes and morphology of spits along southern Karnataka, west coast of India: A remote sensing and statistics-based approach," Geomorphology, vol. 120, no. 3-4, 2010, pp. 133-52.

[3] B.D.K.A.K.S. Jayappa, "Shoreline change rate estimation and its forecast : remote sensing , geographical information system and statistics-based approach," Int. J. Environ. Sci. Technol., vol. 11, 2014, pp. 395-416.

[4] U. Natesan, A. Parthasarathy, R. Vishnunath, G. E. J. Kumar, and V. A. Ferrer, "Monitoring Longterm Shoreline Changes along Tamil Nadu, India Using Geospatial Techniques," Aquat. Procedia Int. Conf. WATER Resour. Coast. Ocean Eng., vol. 4, no. Icwrcoe, 2015, pp. 325-32.

[5] P.B. Cisneros Linares, "Sea level rise impacts in coastal Zones: Soft measures to cope with it," Dalhousie J. Interdiscip. Manag., vol. 8, no. August, 2012, doi: 10.5931/djim.v8i2.282.

[6] M.D. Kudale, a V Mahalingaiah, and B. R. Tayade, "Use of sand-filled geotextile tubes for sustainable coastal protection-case studies in Indian scenario," Indian J. Mar. Sci., vol. 2014, no. July, pp. 5-7, 2014.

[7] S.C. Lee, R. Hashim, S. Motamedi, and K. Song, "Utilization of Geotextile Tube for Sandy and Muddy Coastal Management : A Review," Sci. world J., vol. 2014, p. 9.

[8] L.E. Harris and J.W. Sample, "The Evolution of Multi-Celled Sand-Filled Geosynthetic Systems for Coastal Protection and Surfing Enhancement," Reef J., vol. 1, no. 1, 2009, pp. 1-15.

[9] Y.H. Faure, C.C. Ho, R.H. Chen, M. Le Lay, and J. Blaza, "A wave flume experiment for studying erosion mechanism of revetments using geotextiles," Geotext. Geomembranes, vol. 28, no. 4, 2010, pp. 360-73.

[10] E.M. Palmeira and J. Tatto, "Behaviour of geotextile filters in armoured slopes subjected to the action of waves," Geotext. Geomembranes, vol. 43, no. 1, 2015, pp. 46-55.

[11] J.R. Weggel, "On the Stability of Shore-Parallel Geotextile Tubes for Shore Protection," Geosynth. Res. Dev. Prog., 2005.

[12] K. Yasuhara and J. Recio-Molina, "Stability of modified geotextile wrap-around revetments (GWR) for coastal protection," Geosynth. Int., vol. 12, no. 5, 2005, pp. 260-8.

[13] H. Moayedi, B.B.K. Huat, T.A.M. Ali, Z. Bakhshipor, and M. Ebadi, "Comparison of geotube and stone cemented wall stability as coastal protection system [case study and 2D limit equilibrium and FEM modeling analysis]," Aust. J. Basic Appl. Sci., vol. 5, no. 7, pp. 1-6, 2011, [Online]. Available:

http://www.scopus.com/inward/record.url?eid=2-s2.0-79960484678&partnerID=tZOtx3y1.

[14] K.K. Dabir V.V, "Geosynthetics in coastal protection: An Indian Overview," in Proceedings of International Conference on Hydraulics, Water Resources and Coastal Engineering (Hydro2016), CWPRS Pune, India, 2016, no. December, pp. 683-9.

[15] E.C. Shin and Y.I. Oh, "Coastal erosion prevention by geotextile tube technology," Geotext. Geomembranes, vol. 25, no. 4-5, 2007, pp. 264-77.

[16] S. Corbella and D.D. Stretch, "Geotextile sand filled containers as coastal defence: South African experience," Geotext. Geomembranes, vol. 35, 2012, pp. 120-30.

[17] K. Yasuhara and J. Recio-Molina, "Geosynthetic-wrap around revetments for shore protection," Geotext. Geomembranes, vol. 25, no. 4-5, 2007, pp. 221-32.

[18] H. Wu et al., "Review of application and innovation of geotextiles in geotechnical engineering," Materials (Basel)., vol. 13, no. 7, 2020, pp. 1-21.

[19] K.G. Shirlal and R. R. Mallidi, "Physical model studies on stability of geotextile sand containers," Procedia Eng. 8th Int. Conf. Asian Pacific Coasts, vol. 116, no. 1, 2015, pp. 567-4.

[20] V.A.N. Soysa, D.M.D.T.B. Dassanayake, and H. Oumeraci, "Hydraulic Stability of Submerged GSC structures," vol. XXXXV, no. 4, 2012, pp. 31-40.

[21] S. Neelamani and P.V. Prasad Raju, "Wave interaction with parabolic corrugated and perforated wave absorbers," ISH J. Hydraul. Eng., vol. 10, no. 1, 2004, pp. 19-32.

[22] S. Zhu and A.T. Chwang, "Investigations on the reflection behaviour of a slotted seawall," Coast. Eng., vol. 43, 2001, no. 2, pp. 93-104.

[23] X. Jia, H. Liu, and B. Xu, "An experimental study on dynamic response of geotextile structures in regular waves," Procedia Eng. 8th Int. Conf. Asian Pacific Coasts, vol. 116, no. 1, pp. 842-8.

[24] M. Muttray and B. Reedijk, "Design of Concrete Armour Layers," Ocean Coast. Manag., no. October, 2008, pp. 1-17.

[25] T. Karti, "Design of seawall 1," vol. 3, no. 4, 2018, pp. 283-92.

[26] U. S. Army corps of Engineers, "SHORE PROTECTION MANUAL - Volume I," 1984. doi: 10.5962/bhl.title.47830.

[27] W. P. Hornsey, J. T. Carley, I. R. Coghlan, and R. J. Cox, "Geotextile sand container shoreline protection systems: Design and application," Geotext. Geomembranes, vol. 29, no. 4, 2011, pp. 425-39.

[28] H. O. and G. H. Katja Werth, Juan Recio, "Hydraulic permeability of structures made of geotextile sand containers (gsc-structures) - laboratory tests and results," Coast. Eng, 2008., pp. 3793-804.